Supplemental Information for:

Dual substitution strategy to enhance Li^+ ionic conductivity in $Li_7La_3Zr_2O_{12}$ solid electrolyte

Authors

Lucienne Buannic[1*], Brahim Orayech[1], Juan-Miguel López Del Amo[1], Javier Carrasco[1], Nebil A. Katcho[1], Frederic Aguesse[1], William Manalastas[1], Wei Zhang[1,2], John Kilner[1,3], Anna Llordés[1,2*]

1. CIC EnergiGUNE, Parque Tecnológico de Álava, 48, 01510 Miñano, Álava, Spain

2. IKERBASQUE, The Basque Foundation for Science, 48013 Bilbao, Spain

3. Department of Materials, Imperial College, London SW7 2AZ, U.K.

* contact authors: lbuannic@cicenergigune.com; allordes@cicenergigune.com

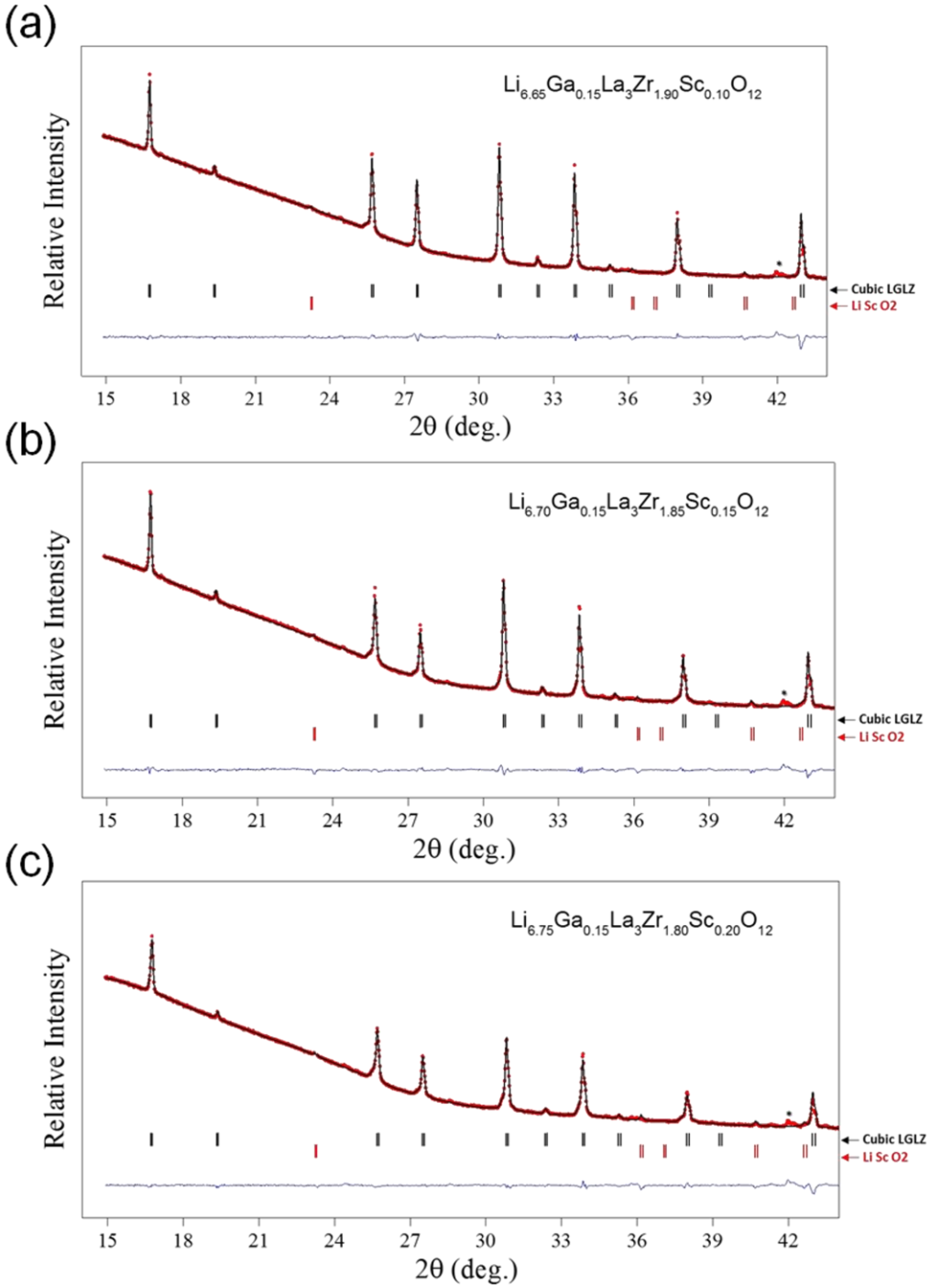

Supplemental Figure S1. *Rietveld refinements of (a) LGLZ_Sc10, (b) LGLZ_Sc15, and (c) LGLZSc_20. The red dots correspond to the experimental XRD pattern, the black line to the calculated pattern, and the blue line to the difference between both patterns. The bars in the lower part of the graphics represent the Bragg peak positions associated with the cubic LGLZ phase ($Ia\bar{3}d$ space group) and the $LiScO_2$ secondary phase present in small amount. The asterisks denote the contribution from the sample holder.*

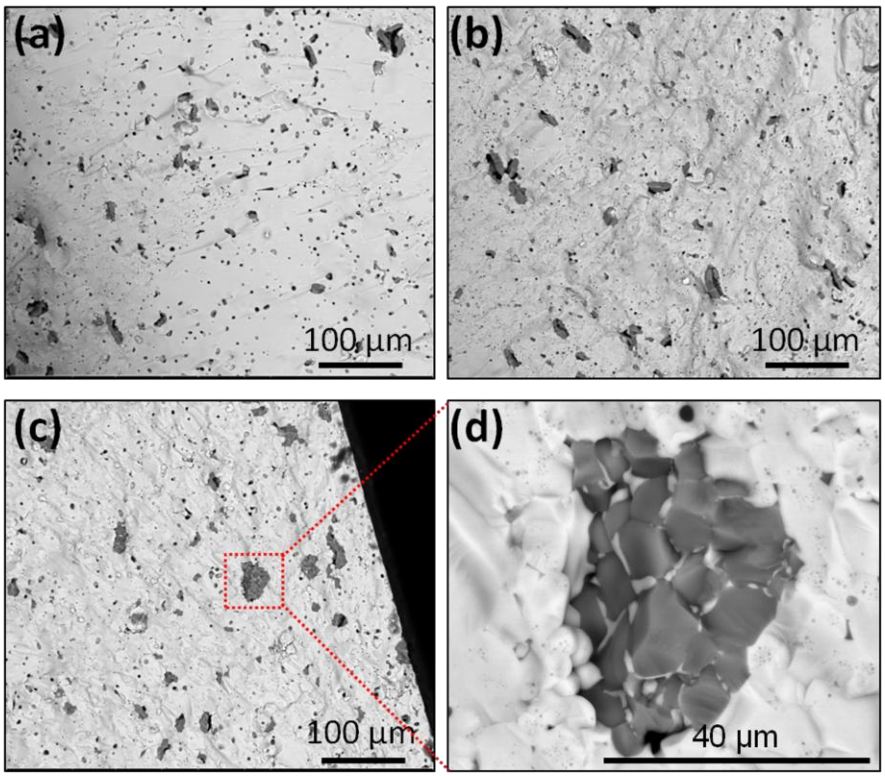

Supplemental Figure S2. *Back scattering electron microscopy of the cross section of (a) LZLG_Sc10, (b) LZLG_Sc15, and (c) LZLG_Sc20 showing the increasing content of secondary phase (dark grey areas). (d) enlarged area highlighted in(c) showing the secondary phase.*

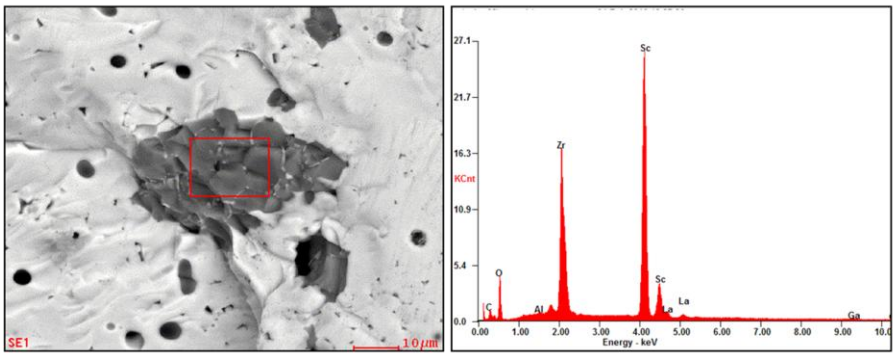

Element	Wt%	At%
CK	05.51	13.92
OK	27.78	52.75
AlK	00.21	00.24
ZrL	30.69	10.22
ScK	32.60	22.03
LaL	02.61	00.57
GaK	00.60	00.26

Supplemental Figure S3. *SEM-EDS analysis of the secondary phase observed in LGLZ_Sc20 with ZAF correction applied.*

Supplemental Table S1. *Averages of SEM-EDS and STEM-EDS for the secondary phase Zr-substituted $LiScO_2$ observed by backscattering imaging.*

Secondary phase		**La:Sc**	**Zr:Sc**	**Ga:Sc**	**Al:Sc**
SEM-EDS					
LGLZ_Sc10	$Li_{6.65}Ga_{0.15}La_3Zr_{1.90}Sc_{0.10}O_{12}$	0.02(1)	0.28(1)	0.01(0)	0.01(0)
LGLZ_Sc15	$Li_{6.70}Ga_{0.15}La_3Zr_{1.85}Sc_{0.15}O_{12}$	0.01(0)	0.28(0)	0.01(0)	0.01(0)
LGLZ_Sc20	$Li_{6.75}Ga_{0.15}La_3Zr_{1.80}Sc_{0.20}O_{12}$	0.03(0)	0.46(0)	0.01(0)	0.01(0)
STEM-EDS					
LGLZ_Sc20	$Li_{6.75}Ga_{0.15}La_3Zr_{1.80}Sc_{0.20}O_{12}$	0.04(1)	0.62(5)	0.007(3)	0.001(3)

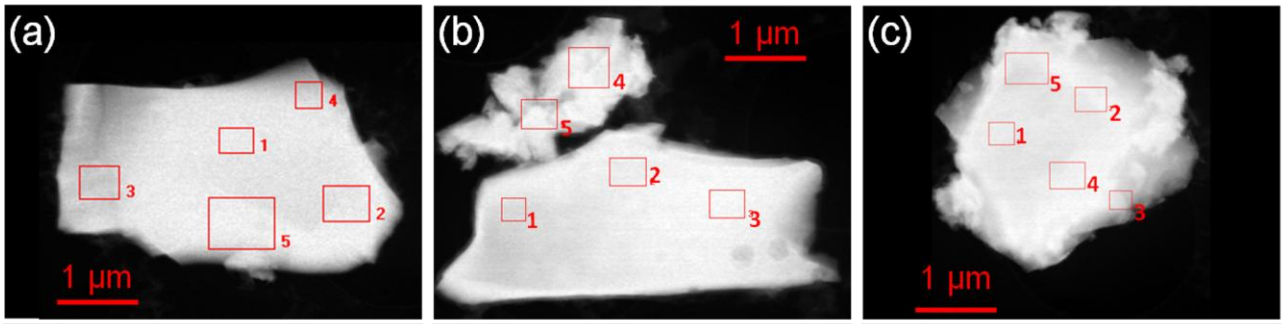

Area	La(L)	Zr(K)	Ga(K)	Sc(K)	Al(K)
1	3.00(6)	2.46(9)	0.13(2)	0.12(2)	-
2	3.00(6)	1.91(7)	0.17(2)	0.14(1)	-
3	3.00(10)	2.77(13)	0.23(4)	-	-
4	3.00(55)	4.1(1.0)	-	-	-
5	3.00(7)	1.65(9)	0.11(2)	-	-

Area	La(L)	Zr(K)	Ga(K)	Sc(K)	Al(K)
1	3.00(5)	1.91(6)	0.28(1)	0.06(2)	-
2	3.00(5)	1.79(7)	0.16(2)	0.07(1)	-
3	3.00(5)	2.40(7)	0.27(1)	0.17(2)	-
4	3.00(6)	2.27(8)	0.25(1)	0.07(1)	0.05(1)
5	3.00(6)	2.06(8)	0.08(2)	-	-

Area	Sc(K)	Zr(K)	La(L)
1	1.00(2)	0.68(2)	-
2	1.00(2)	0.44(2)	-
3	1.00(3)	0.63(3)	-
4	1.00(2)	0.56(2)	-
5	1.00(2)	0.77(2)	0.21(1)

Supplemental Figure S4. *STEM-EDS elemental analysis of isolated particles of LGLZ_Sc20 representative of (a) and (b) garnet phase, and (c) Zr-substituted $LiScO_2$ secondary phase . The uncertainty in area 4 of (a) was too high to be considered as a reliable result.*

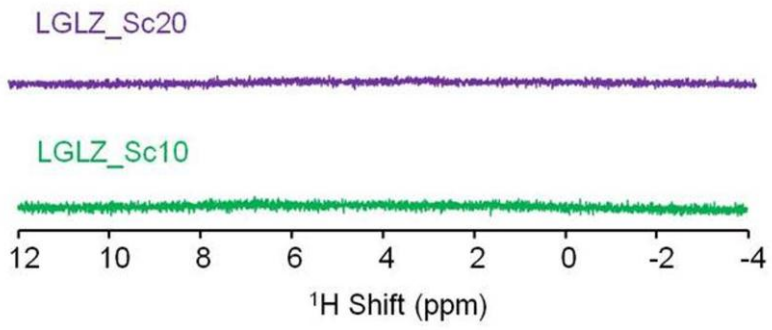

Supplemental Figure S5. *^1H NMR spectra of (a) LGLZ_Sc10 and (b) LGLZ_Sc20.*

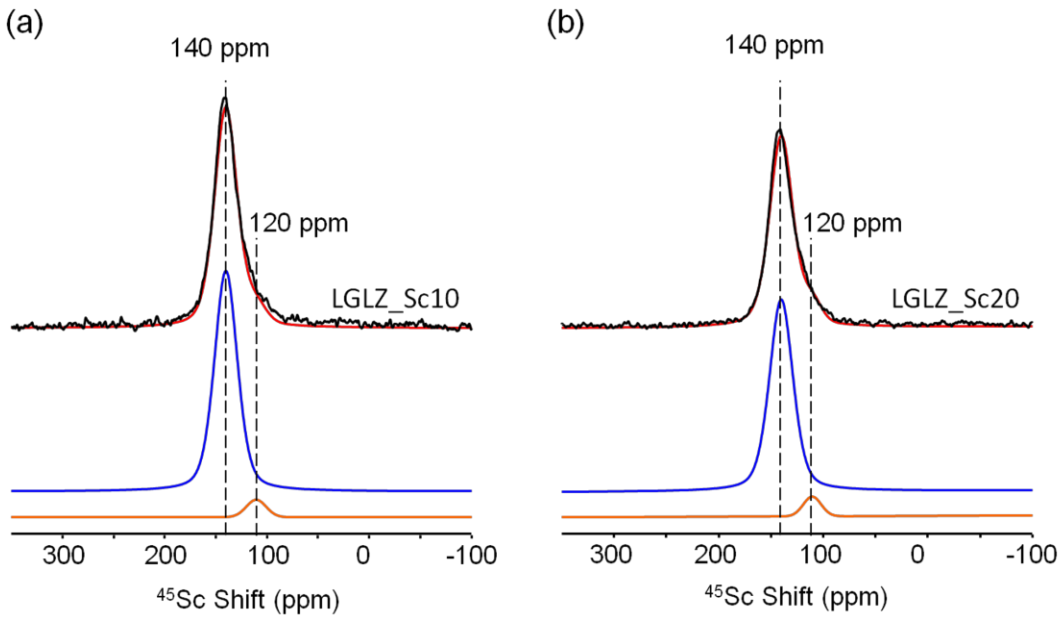

Supplemental Figure S6. *Deconvolution of the ^{45}Sc NMR spectra of (a) LGLZ_Sc10 and (b) LGLZ_Sc20.*

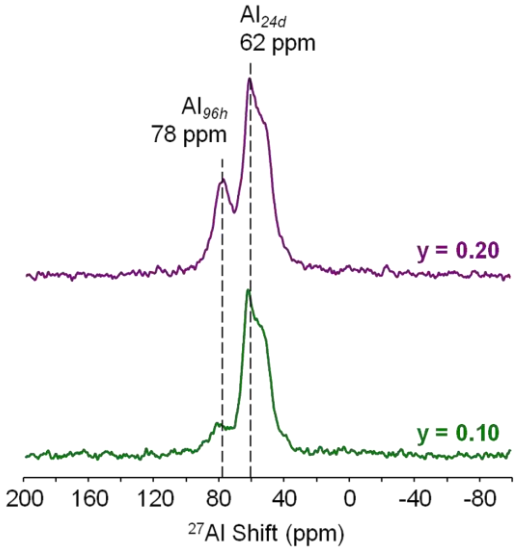

Supplemental Figure S7. *^{27}Al NMR spectra of (a) LGLZ_Sc10 and (b) LGLZ_Sc20.*

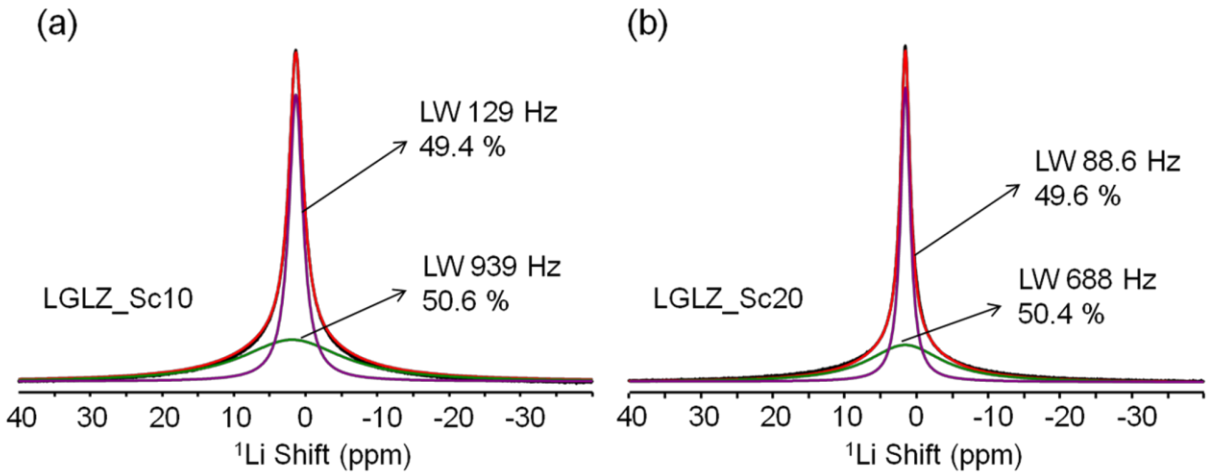

Supplemental Figure S8. *Deconvolution of the ^{7}LiNMR spectra of (a) LGLZ_Sc10 and (b) LGLZ_Sc20.*

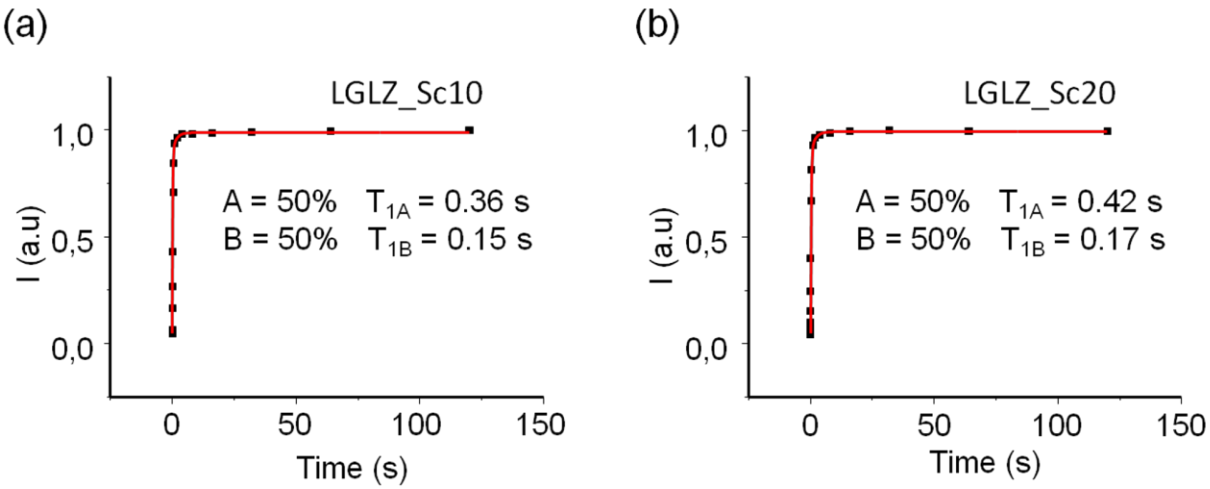

Supplemental Figure S9. *^{7}Li T_1 relaxation curves for (a) LGLZ_Sc10 and (b) LGLZ_Sc20.*

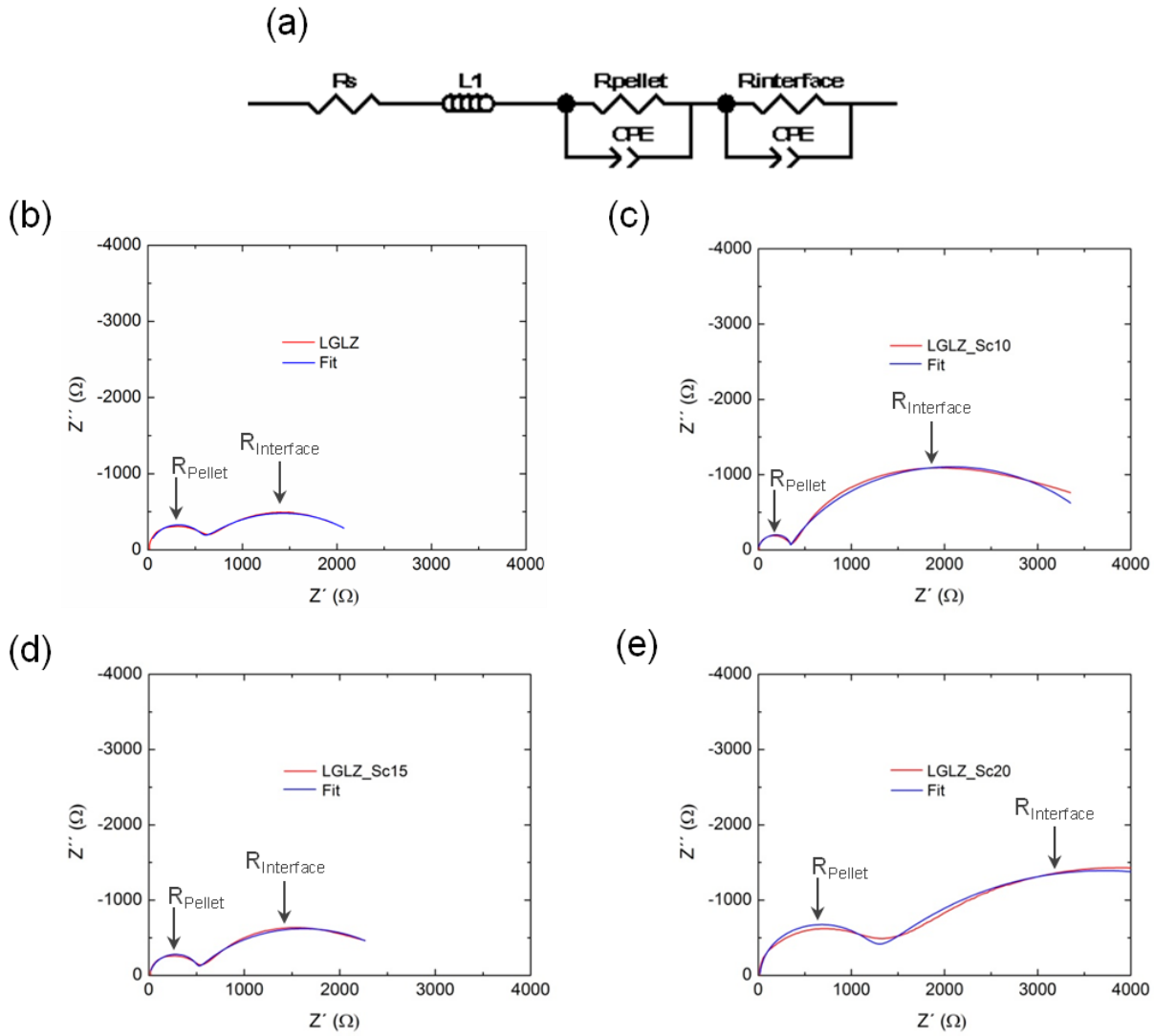

Supplemental Figure S10. *(a) Equivalent circuit used for fitting Nyquist plots with R_{Pellet} being the total (bulk + grain) resistance of the garnet sample and $R_{Interface}$ the resistance between the garnet and the Li electrodes. Fit obtained for the 300K Nyquist plots of (b) LGLZ, (c) LGLZ_Sc10, (d) LGLZ_Sc15, and (e) LGLZ_Sc20.*